Visualization of a Recurrent Carcinoid Tumor and an Occult Distant Metastasis by Technetium-99m-Sestamibi

Shobha P. Desai and David L. Yuille

Nuclear Medicine Department, St. Luke's Medical Center, Milwaukee, Wisconsin

We present a case of atypical carcinoid that showed avid uptake of sestamib in a recurrent bronchial carcinoid tumor and a solitary, unsuspected, occult, bony metastatic lesion in the distal femur. As carcinoid tumors are known to be vascular, we suspect that its avidity for sestamibi is secondary to increased blood flow, although other factors such as the transmembrane potentials of plasma and mitochondrial membranes and relative number of mitochondria present in the cells of this carcinoid tumor, may have also played a role.

J Nucl Med 1993; 34:1748–1751

Bronchial carcinoid tumors usually are benign and have a good prognosis with low incidence of metastases, but some run a rapid course with metastatic spread and are histologically labeled as "atypical carcinoid tumors." (*1–4*). The pathologic diagnosis of an atypical carcinoid is based on atypical histological features such as notable variability in size and shape of cells, presence of mitosis and polymorphous nucleolar configuration. Metastases were usually absent at the time of diagnosis, but a metastasizing potential was recognized.

CASE REPORT

The patient is a 76-yr-old white female who had a left upper lobectomy in 1988 for an atypical carcinoid tumor metastatic to several lymph nodes at the time of diagnosis. She subsequently received 6 mo of chemotherapy and remained disease-free through March of 1992. A chest radiograph taken on September 1, 1992, revealed a new soft-tissue density lateral to the aortic arch that was confirmed on CT scan. A follow-up sestamibi tumor scan was performed on September 15, 1992, after intravenous administration of 30 mCi of ^{99m}Tc-sestamibi because of clinical interest generated by published reports of tumor scanning with sestamibi. The whole-body scan was performed 30 min postinjection on a whole-body camera, at a table speed of 15–17 cm/min for a total imaging time of 15 min. SPECT images of chest and abdomen were obtained on a dual-head Rota camera equipped with ultra-high resolution collimators. For the SPECT study, a 64 × 64 matrix was used and data were acquired over 360° in 120 angular views of 15 sec each using a pseudocontinuous step-and-shoot data acquisition method developed at this institution.

The scan revealed an ovoid area of increased activity adjacent to the superolateral aspect of the aortic arch corresponding to a known tumor mass seen on CT scan. A small focal area of moderately increased activity consistent with a metastatic focus was noted in the medial aspect of the distal right femoral metaphysis. A bone scan performed for a metastatic workup showed a solitary bone lesion involving the distal right femoral metaphysis medially precisely in the same location as that seen on sestamibi tumor scan. The patient underwent CT-guided biopsy of the right femoral lesion. Microscopy of the tumor biopsy showed irregular nests of cells with increased nuclear cytoplasmic ratio, moderate pleomorphism, hyperchromatism and moderate amount of cytoplasm consistent with metastatic atypical carcinoid tumor. Unfortunately, the number of mitochondria percent could not be determined in this case since it is difficult to assess the number of mitochondria by light microscopic appearance. Electron microscopy could not be performed because of the small tissue sample obtained by biopsy. Except for the uncommon oncocytic carcinoid tumor, both typical and atypical carcinoid tumors do not contain an increased number of mitochondria, although there is some variation in mitochondrial concentration from tumor to tumor (*6*).

DISCUSSION

Neuroendocrine carcinomas of the lung constitute approximately 25% of all lung tumors (*7*), including classic carcinoid (Kulchitsky-cell carcinoma [KCC I], atypical carcinoid (KCC II), or small-cell carcinoma (KCC III)). Precise histopathological classification is important because treatment and prognosis among the three groups of tumors differ significantly (*8*). In most reported series, KCC II lesions constitute 25% of carcinoid tumors (*9*). Lymph node metastases occur in 3% of patients with KCC I tumors and in 40%–50% of patients with KCC II tumors (*10,11*). Bronchoscopy is useful in the diagnosis of 60%–80% of KCC I tumors, but the bronchoscopic diagnosis of KCC II tumors is more difficult due to inability to visualize some of these tumors (*9,12*).

Bronchial carcinoids are particularly slow growing, thus resection generally leads to an excellent prognosis (*13*).

Received Feb. 10, 1993; revision accepted June 17, 1993.

For correspondence or reprints contact: Shobha P. Desai, MD, Nuclear Medicine Department, St. Luke's Medical Center, 2900 W. Oklahoma Ave., P.O. Box 2901, Milwaukee, WI 53201-2901.

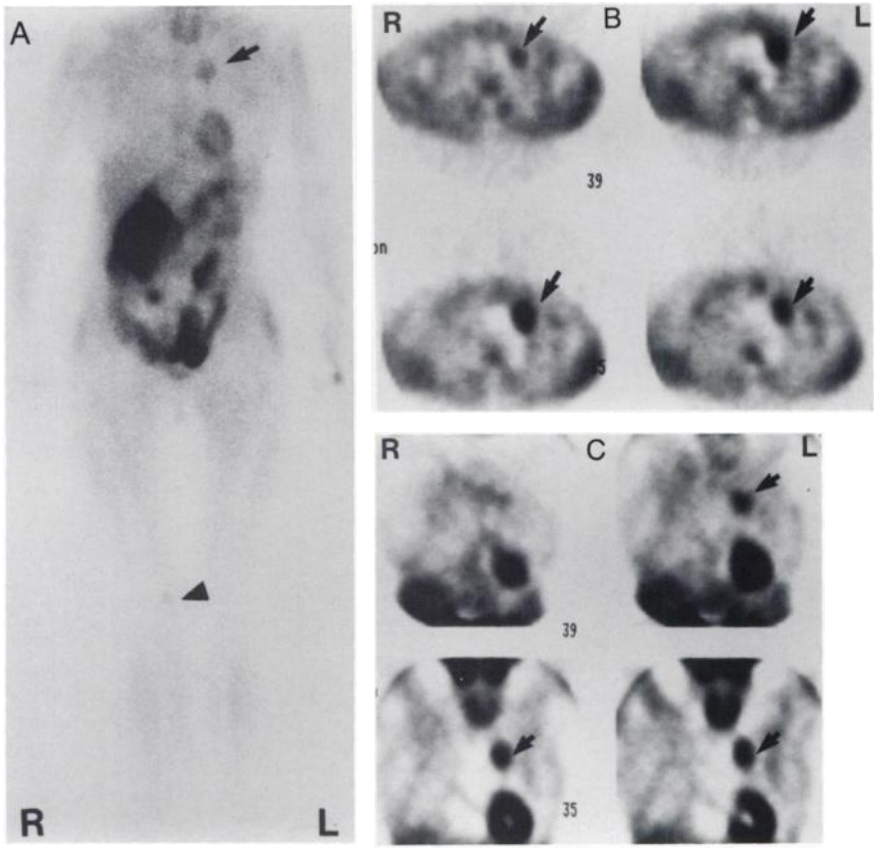

FIGURE 1. Sestamibi tumor scan after administration of 30 mCi of MIBI. Anterior whole-body planar view (A) demonstrates increased MIBI uptake in the thoracic tumor (arrow) and faint increased uptake in distal right femoral metaphysis (arrowhead) compatible with solitary bony metastasis. Transverse (B) and coronal (C) SPECT images of the thorax demonstrate intense increased activity in the tumor (arrow) adjacent to the aortic arch (photogenic area). Normal MIBI uptake is seen in thyroid, heart and bone marrow of the spine.

Malignancy is not determined by histologic features but by the appearance of metastases which may occur up to 10 yr after apparently successful treatment of the primary lesions (*14*). Smith (*15*) and many others feel that histopathology alone offers no prognostic value in bronchial carcinoid. A review of 60 patients by Rea et al. (*16*) suggests that long-term survival is high, 93% at 5 yr and 89.6% at 10 yr, in the case of typical carcinoids. In contrast, atypical carcinoids had significant malignant potential with a 5-yr survival of 66% and 10-yr survival of 60%. The negative prognosis related to lymph node metastases has been reported by many authors (*16–18*).

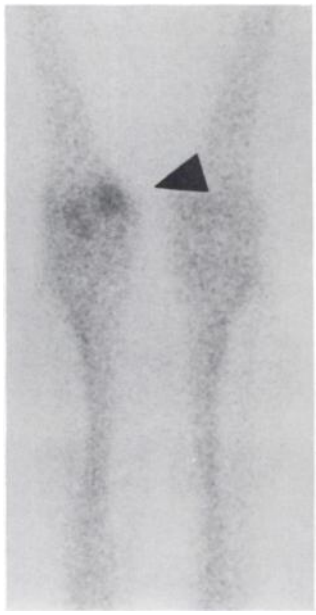

FIGURE 2. Anterior view of knee joints after administration of 20 mCi of ^{99m}Tc-MDP shows focal area of increased activity in the distal right femoral metaphysis. In the absence of a sestamibi tumor scan finding, this abnormality could have been easily misinterpreted as degenerative changes.

Hexakis (methoxyisobutylisonitrile) technetium (I) (Tc-MIBI) is an excellent myocardial perfusion agent (*19,20*). Technetium-MIBI belongs to a class of ^{99m}Tc-based lipophilic cationic agents whose myocardial distribution is proportional to regional blood flow. Once intracellular, it is sequestered largely within mitochondria (*21*). Significant uptake in a broad range of organs, including liver, skeletal muscle, lung, thyroid, and kidney, was demonstrated in animals and humans. Recently, its tumor imaging properties have undergone investigation. Sestamibi uptake has been reported in lung cancers (*22,23*), breast cancer, lymphomas, mediastinal and pulmonary metastasis from thyroid cancer (*24*), peripheral soft tissue and bone sarcomas (*25*), and undifferentiated mesenchymal tumor (*26*). Ramanathan et al. (*27*) used ^{99m}Tc-MIBI for visualization of suppressed thyroid tissue, and preliminary reports indicate that ^{99m}Tc-MIBI also localizes in parathyroid adenomas (*28*).

It has been reported that ^{99m}Tc-MIBI accumulates within mitochondria and cytoplasm of cells on the basis of electrical potentials generated across the membrane bilayers (*29–31*) of both plasma and mitochondrial membranes. Since malignant tumors maintain higher (more negative) mitochondrial and plasma transmembrane potentials secondary to their increased metabolic requirements, this

should cause increased accumulation of MIBI in malignant tumors (*30*) as opposed to other types of tissues. It has also been reported that metabolic blockade with metabolic inhibitors such as rotenone and iodoacetate could depress MIBI cellular uptake (*32*). Interestingly, the equilibrium intracellular concentration of sestamibi has also recently been found to be inversely related to the degree of expression of P-glycoprotein, an ancient pump protein responsible for the development of multi-drug resistance to chemotherapeutic agents (*33*).

While myocardial uptake is constant over 1 hr, tumor uptake first increases and then decreases with time (*24*). Reports have suggested that the optimum imaging time for MIBI uptake is between 30–60 min after injection. Preliminary reports of human imaging with ^{99m}Tc-MIBI have shown uptake more than 50% higher in tumor than in normal tissue (*22–24*). Uptake in benign tumors is uncommon, but does occur in adenomas of the breast, thyroid, and parathyroid glands. Caner et al. (*34*) believe that MIBI uptake is more closely related to factors such as blood flow, tumor necrosis, metabolic demand and mitochondrial activity rather than the nature of the lesion. Their data suggest that radiotherapy and/or chemotherapy significantly inhibit the uptake of MIBI and can thus be used to evaluate the effectiveness of therapy.

In our patient, sestamibi uptake by a recurrent carcinoid tumor and unsuspected bony metastasis is important for two reasons. First, the finding of an occult metastasis was quite important in patient management since this patient received chemotherapy rather than surgery or radiation therapy as initially planned. Second, because of the location of the metastatic lesion near the knee joint, the patient's bone scan could easily have been misinterpreted as a degenerative change rather than a metastatic lesion. Instead, the sestamibi uptake led to a follow-up CT scan and eventual biopsy of the lesion.

Technetium-MIBI may have a potential role in evaluating patients with malignancies, particularly of the lung and mediastinum. This case report illustrates the usefulness of sestamibi tumor scanning in initial evaluation of carcinoid tumors that are difficult to assess for malignancy on pathological grounds alone. As carcinoids are vascular tumors, it may be anticipated that sestamibi will prove to be of significant value in a larger series of these tumors, although further work is required.

ACKNOWLEDGMENTS

The authors thank Ms. Camille Dykas and Ms. Jean Lemanski for preparing the manuscript, and R.F. Anderson, CNMT for technical assistance. We also thank W.G. Doos, MD for reviewing this case and furnishing us with histopathologic details.

REFERENCES

1. Von Albertini A. Pathologisch-anatomisches kurzreferat zum thema lungenkrebs. *Schweiz Med Wochenschr* 1951;81:659.
2. Bensch KG, Corrin B, Pariente R, Spencer H. Oat-cell carcinoma of the lung: its origin and relationship to bronchial carcinoid. *Cancer* 1968;22:1163.
3. Goodner JT, Berg JW, Watson WL. The nonbenign nature of bronchial carcinoids and cylindromas. *Cancer* 1961;14:539.
4. McBurney RP, Kirklin JW, Woolner LB. Metastasizing bronchial adenomas. *Surg Gynecol Obstet* 1953;96:482.
5. Engelbreth-Holm J. Benign bronchial adenomas. *Acta Chir Scand* 1944–1945;90:383.
6. Mackay B, Lukeman JM, Ordonez NG. Tumors of the lung. In: *Series major problems in pathology, volume 24*. Philadelphia: W.B. Saunders Company, 1991:246–284.
7. Yesner R. Small cell tumors of the lung. *Am J Surg Pathol* 1983;7:775–785.
8. Wilkins EW, Grillo HC, Moncure AC, Scannell JG. Changing times in surgical management of bronchopulmonary carcinoid tumor. *Ann Thorac Surg* 1984;38:339–344.
9. McCaughan BC, Martini N, Bains MS. Bronchial carcinoids: review of 124 cases. *J Thorac Cardiovasc Surg* 1985;89:8–17.
10. Mills SE, Cooper PH, Walker AN, Kron IL. Atypical carcinoid tumor of the lung: a clinicopathologic study of 17 cases. *Am J Surg Pathol* 1982;6:643–654.
11. Mark EJ, Ramirez JF. Peripheral small-cell carcinoma of the lung resembling carcinoid tumor: a clinical and pathologic study of 14 cases. *Arch Pathol Lab Med* 1985;109:263–269.
12. Bertelsen S, Aasted A, Lung C, et al. Bronchial carcinoid tumors: a clinicopathologic study of 82 cases. *Scand J Thorac Cardiovasc Surg* 1985;19:105–111.
13. Martensson H, Bottcher B, Hambraeus G, Sundler F, Willen H, Nobin A. Bronchial carcinoids: an analysis of 91 cases. *World J Surg* 1987;11:356–364.
14. Bensch KG, Gordon GB, Miller LR. Electron microscopic and biochemical studies on the bronchial carcinoid tumor. *Cancer* 1965;18:592–602.
15. Smith RA. Bronchial carcinoid tumors. *Thorax* 1969;24:43.
16. Rea F, Binda R, Spreafico G, et al. Bronchial carcinoids: a review of 60 patients. *Ann Thorac Surg* 1989;47:412–414.
17. Turnbull AD, Huvos AG, Goodner JT, Beattie EJ Jr. The malignant potential of bronchial adenoma. *Ann Thorac Surg* 1972;14:453.
18. Goldstraw P, Lamb D, McCormack RJM, Walbaum PR. The malignancy of bronchial adenoma. *J Thorac Cardiovasc Surg* 1976;72:309.
19. Wackers FJ-Th, Berman DS, Maddahi J, et al. Technetium-99m-hexakis 2-methoxyisobutylisonitrile: human biodistribution, dosimetry, safety, and preliminary comparison to thallium-201 for myocardial perfusion imaging. *J Nucl Med* 1989;30:301–311.
20. West DJ, Najim YC, Mistry R, Clarke SE, Fogelman I, Maisey MN. The localization of myocardial ischaemia with technetium-99m methoxy isobutyl isonitrile and single photon emission computed tomography. *Br J Radiol* 1989;62:303–313.
21. Beller GA, Watson DD. Physiological basis of myocardial perfusion imaging with the technetium-99m agents. *Semin Nucl Med* 1991;21:173–181.
22. Hassan IM, Sahweil A, Constantinides C, et al. Uptake and kinetics of Tc-99m-hexakis 2-methoxy isobutyl isonitrile in benign and malignant lesions in lungs. *Clin Nucl Med* 1989;14:333–340.
23. Muller SP, Reiners C, Paas M, et al. Tc-99m MIBI and Tl-201 uptake in bronchial carcinoma [Abstract]. *J Nucl Med* 1989;30:845.
24. Muller S, Guth-Tougelides B, Creutzig H. Imaging of malignant tumors with Tc-99m-MIBI SPECT [Abstract]. *J Nucl Med* 1987;28:562.
25. Caner B, Kitapci M, Aras T, Erbengi G, Ugur O, Bekdik C. Increased accumulation of hexakis (2-methoxy isobutyl isonitrile) technetium (I) in osteosarcoma and its metastatic lymph nodes. *J Nucl Med* 1991;32:1977–1978.
26. Caner B, Kitapci M, Erbengi G, et al. Increased accumulation of Tc-99m-MIBI in undifferentiated mesenchymal tumor and its metastatic lung lesions. *Clin Nucl Med* 1992;17:144–145.
27. Ramanathan P, Patel RB, Subrahmanyam N, et al. Visualization of suppressed thyroid tissue by technetium-99m-tertiarybutyl isonitrile (^{99m}Tc-TBI): an alternative to post-TSH stimulation scanning. *J Nucl Med* 1990;31:1163–1165.
28. Coakley AJ, Kettle AG, Wells CP, O'Doherty MJ, Collins REC. Technetium-99m-sestamibi: a new agent for parathyroid imaging. *Nucl Med Comm* 1989;10:791–794.
29. Delmon-Moingeon LI, Piwnica-Worms D, Van den Abbleele AD, et al. Uptake of cation hexakis (2-methoxyisobutyl isonitrile) technetium-99m by human carcinoma cell lines in vitro. *Cancer Res* 1990;50:2198–2202.
30. Chiu ML, Kronauge JF, Piwnica-Worms D. Effect of mitochondrial and plasma membrane potentials on accumulation of hexakis (2-methoxyisobutylisonitrile) technetium (I) in cultured mouse fibroblasts. *J Nucl Med* 1990;31:1646–1653.
31. Piwnica-Worms D, Chiu ML, Kronauge JF. Membrane potential-sensitive

retention of Tc-99m MIBI in cultured chick heart cells [Abstract]. *Radiology* 1989;173:281.
32. Piwnica-Worms D, Kronauge JF, Delmon L, et al. Effect of metabolic inhibition on technetium-99m-MIBI kinetics in cultured chick myocardial cells. *J Nucl Med* 1990;31:464–472.
33. Piwnica-Worms D, Chiu ML, Budding M, et al. Functional Imaging of multidrug-resistant, P-Glycoprotein with an organotechnetium complex. *Cancer Res* 1993;53:977–984.
34. Caner B, Kitapcl M, Unlu M, et al. Technetium-99m-MIBI uptake in benign and malignant bone lesions: a comparative study with technetium-99-MDP. *J Nucl Med* 1992;33:319–324.

(continued from page 5A)

FIRST IMPRESSIONS

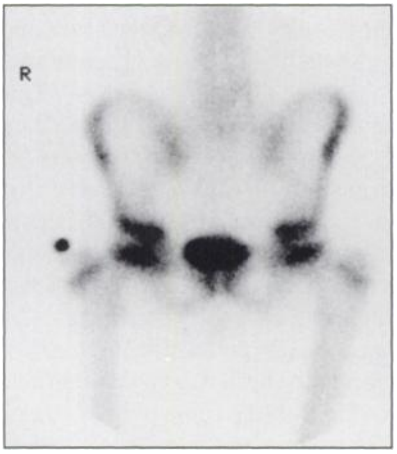

FIGURE 1. Anterior view of the pelvis and hips 3 hr following injection of ^{99m}Tc-HDP. Intense focal uptake is shown over the superior aspect of the greater trochanter on the left side.

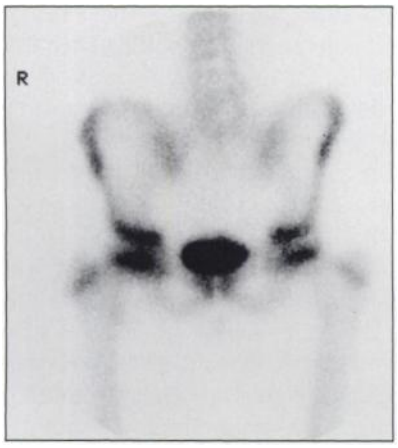

FIGURE 2. Repeat view of the pelvis and hips after emptying the patient's pockets.

PURPOSE

A 13-yr-old girl with old Perthes disease, who had undergone a previous osteotomy of the left femoral neck three years earlier, was continuing to have left hip pain. She was referred for follow-up bone scan to determine whether the origin of pain was physical or nonorganic.

Blood-pool images showed no abnormality. Initial 3-hr views of the pelvis demonstrated a site of intense focal uptake at the superior aspect of the greater trochanter of the right femur (Fig. 1). When the technologists questioned the patient about the pain site, they considered the possibility of contamination. Asked to empty her pockets, the patient produced a cotton wool swab that had been used on the venapuncture site following administration of the radiopharmaceutical. Repeat image views showed no abnormality (Fig. 2).

This case demonstrates that patients should not be permitted to dispose of swabs following administration of radiopharmaceuticals and should certainly not be allowed to leave the hospital with contaminated swabs. The resulting artifact could affect final interpretation of images.

TRACER

470 MBq (12.7 mCi) of ^{99m}Tc-HDP.

ROUTE OF ADMINISTRATION

Intravenously.

TIME AFTER INJECTION

Immediate blood-pool and 3-hr planar views, each consisting of 700 k counts.

INSTRUMENTATION

IGE 400ac/Starport gamma camera.

CONTRIBUTORS

Alan Perkins, Mandy Blaze, Simon Lawes and Kevin Blackband.

INSTITUTION

Nuclear Medicine Clinic, Department of Medical Physics, University Hospital, Nottingham, UK.